Time Evolution of the Rotational Transform Profile in Current-Carrying LHD Plasmas

Yuji NAKAMURA, Kiyomasa WATANABE[1], Yoshiro NARUSHIMA[1], Katsumi IDA[1],
Mikiro YOSHINUMA[1], Satoru SAKAKIBARA[1], Hisamichi FUNABA[1], Kazuo KAWAHATA[1],
Masayuki YOKOYAMA[1], Noriyoshi NAKAJIMA[1] and Atsushi FUKUYAMA[2]

Graduate School of Energy Science, Kyoto University, Gokasho, Uji, Kyoto 611-0011, Japan
[1]National Institute for Fusion Science, 322-6 Oroshi-cho, Toki, Gifu 509-5292, Japan
[2]Graduate School of Engineering, Kyoto University, Yoshida, Kyoto, Kyoto 606-8501, Japan

Numerical analysis is performed for a low beta neutral beam heated plasma and a superdense core plasma in the Large Helical Device (LHD) to investigate the time evolution of the rotational transform profile, which is calculated consistently with the three-dimensional magnetohydrodynamics equilibrium. Although there is a considerable amount of noninductive current flow, such as the bootstrap and Ohkawa currents, the inductive current component prevents a rapid change of the rotational transform profile in these plasmas.

1. Introduction

The effort to develop an integrated transport code for helical plasmas, TASK3D, is in progress to understand the confinement physics and to design new experimental plans [1, 2]. The major differences between TASK3D, which is consistent with the three-dimensional (3D) magnetohydrodynamics (MHD) equilibrium for helical plasmas, and a one and half dimensional (1.5D) transport code, which is used for tokamak plasmas, include the neoclassical ripple transport, determination of the (ambipolar) radial electric field, and time evolution of toroidal current profile, which is equivalent to that of the rotational transform profile. In these studies, the time evolution of the rotational transform due to the finite plasma resistivity in a nonaxisymmetric plasma is solved self consistently with 3D MHD equilibria.

Although MHD equilibria can exist for zero net current in helical plasmas, finite net toroidal currents have been observed in many actual experiments, even when the Ohmic current is not driven actively. It is considered that the noninductive currents, such as bootstrap and beam driven currents, are the main component of the net plasma current. However, change in the plasma current due to the noninductive currents induces inverse toroidal electric field, when the plasma resistivity is small and the current penetration time is long. In other word, the inversely induced current is driven so as to suppress the change in the plasma current. Unless the Ohmic current is driven actively by an external circuit, the total net current tends to noninductive as time evolves to the steady state,

author's e-mail: nakamura@energy.kyoto-u.ac.jp

because the inductive current is decayed by the small but finite plasma resistivity. In an LHD plasma, for example, it takes more than 4 s to achieve the stationary state [3]. Since the rotational transform profile, which has important roles in the MHD stability and confinement, is sensitive to the net plasma current, it is indispensable to clarify the effect of inductive component of the plasma current qualitatively. In our previous study [3], MHD equilibrium and noninductive current profile are fixed in time during the calculation of the rotational transform profile. However, numerical problems were encountered at the plasma center and the plasma boundary when we updated the MHD equilibrium and noninductive current at some time intervals.

In the present study, the above numerical problems that arose from the boundary condition are removed by changing the difference scheme. We apply this simulation code to the LHD experiments in which the direction of neutral beam (NB) injection is switched from the counterdirection to the co-direction, and clarify the role of inductive plasma current profile quantitatively. We also apply this analysis to a superdense core (SDC) plasma in LHD to estimate the rotational transform profile in the SDC plasma.

2. Time Evolution of the Rotational Transform

A conservation equation for the rotational transform ι is derived from the contravariant component of Faraday's law [4]:

$$\frac{\partial \iota}{\partial t} = \frac{1}{\phi'} \left[\left. \frac{\partial \phi}{\partial t} \right|_\rho \frac{\partial \iota}{\partial \rho} + \frac{\partial}{\partial \rho} \left(\frac{\mathcal{V}'}{\phi'} \langle \boldsymbol{E} \cdot \boldsymbol{B} \rangle \right) \right],$$

where $\phi = \Phi_T/2\pi$, Φ_T is the toroidal magnetic flux, ρ is an arbitrary flux surface label, $\mathcal{V} = V/(2\pi)^2$, V is volume inside the flux surface, and $\langle E \cdot B \rangle$ corresponds to the flux averaged parallel electric field. Primes denotes derivative with respect to ρ. If we use the parallel component of Ohm's law,

$$\langle E \cdot B \rangle = \eta_{\parallel} \left(\langle j \cdot B \rangle - \langle j_{NI} \cdot B \rangle \right),$$

and use the relation between the parallel current density and ι, we can get the diffusion equation of ι [1, 3]. Here, $\eta_{\parallel}$ is the neoclassical parallel resistivity, and $\langle j \cdot B \rangle$ and $\langle j_{NI} \cdot B \rangle$ correspond to the flux averaged parallel current density and noninductive current density, respectively.

In a previous study, we solved the diffusion type equation for the rotational transform that uses $\rho \equiv \sqrt{s}$ as a radial variable, where $s \equiv \Phi_T/\Phi_T^{edge}$ is the toroidal flux normalized by its value at the plasma boundary. The Crank-Nicholson difference scheme was used on a half radial grid point, $\rho = \rho_{j-1/2} \equiv (j - 1/2)\Delta\rho$, where $\Delta\rho$ is an uniform radial grid spacing. The use of half grid points is suitable for the boundary condition at the plasma center. However, there were numerical problems in some cases. The problems arose from two reasons. One is that the interpolation of the MHD equilibrium data calculated on uniform s grids by the VMEC code [5] to those on uniform ρ grids is not sufficiently accurate near the magnetic axis. Another is that numerical instabilities come from the boundary condition at the plasma boundary, which is not defined on the half grid points.

In order to improve numerical stability, we use s as a radial variable in the equation of the rotational transform profile, which now can be written as

$$\frac{\partial \iota}{\partial t} = \left(\frac{\phi_a}{s} \frac{\partial \phi_a}{\partial t} \right) \frac{\partial \iota}{\partial s}$$
$$+ \frac{1}{\phi_a^2} \left\{ \frac{\partial}{\partial s} \left[\eta_{\parallel} \mathcal{V}' \frac{\langle B^2 \rangle}{\mu_0^2} \frac{\partial}{\partial s} (S_{11}\iota + S_{12}) \right] \right.$$
$$\left. + \frac{\partial}{\partial s} \left[\eta_{\parallel} \mathcal{V}' p' (S_{11}\iota + S_{12}) - \eta_{\parallel} \mathcal{V}' \langle J_{NI} \cdot B \rangle \right] \right\}.$$

where $\phi_a = \Phi_T^{edge}/2\pi$, $\langle B^2 \rangle$ is flux surface average of the square of magnetic field strength, p is pressure, and primes denote derivative with respect to s. The susceptance matrix is defined [6] as

$$S_{11} = \mathcal{V}' \left\langle \frac{g_{\theta\theta}}{g} \right\rangle,$$

$$S_{12} = \mathcal{V}' \left\langle \frac{g_{\theta\zeta}(1 + \partial_\theta\lambda) - g_{\theta\theta}\partial_\zeta\lambda}{g} \right\rangle,$$

where λ is a magnetic field stream function defined in the VMEC representation [5]. The rotational transform is related to the toroidal current within the flux surface, $I_T(s)$, through the susceptance matrix as,

$$\iota = \frac{I_T}{\Phi_T' S_{11}} - \frac{S_{12}}{S_{11}}.$$

It should be noted that $S_{12} = 0$ and ι is proportional to the toroidal current in axisymmetric plasmas. For numerical calculations, a finite difference equation is defined on a full grid point, $s = s_j \equiv j\Delta s$, instead of a half grid point to eliminate the numerical difficulty at the plasma boundary. We named this rotational transform calculation code TASK/EI.

The susceptance matrix, $\langle B^2 \rangle$, $\mathcal{V}'$, and p are obtained from the equilibrium data calculated by the VMEC code. Noninductive bootstrap current, beam driven Ohkawa current, and neoclassical parallel resistivity are calculated by the BSC and FIT codes [1, 3]. These data are supplied to TASK/EI, and the rotational transform is evolved during some time interval, which is typically 100 ms for LHD plasmas. In the equation of ι evolution, we assumed that MHD equilibrium quantities such as susceptance matrix are consistent with evolved ι (in this sense, the equation is intrinsically nonlinear), but we also assumed that the change in ι and the resultant change in MHD quantities are negligibly small during the calculation. Then, the updated rotational transform profile along with the experimentally obtained density and temperature profiles are used as inputs of the VMEC code, and noninductive current is re-estimated by the BSC and FIT codes. These procedures are iterated during the simulation.

3. Analysis of Plasma Current in a Low Beta NBI Plasma

Simulation of the rotational transform profile evolution is performed for a low beta NB heated plasma in LHD [1, 3]. Experimentally evaluated density and electron temperature profiles in this plasma are shown in Fig. 1. The electron density profile is obtained by a far infrared ray measurement, and the electron temperature profile by an electron cyclotron emission measurement. Hereafter, the radial coordinate ρ in the figures denotes the square root of s. The volume averaged beta of the plasma evaluated by diamagnetic measurement is less than 0.2%. Observed total toroidal current is shown in Fig. 2. In this experiment, an NB is injected in the counter-direction at first ($t \sim 1$ s), and then the direction of NB injection is switched to the co-direction. In LHD, Ohmic current is not driven actively by the external circuit. The Ohkawa and bootstrap currents, which are estimated by the BSC and FIT codes are also shown in Fig. 2. The inductive and noninductive components of the total current can be estimated experimentally, and good agreement between theoretical and experimental estimations is shown in Ref. [7]. Therefore, we use the theoretical estimation in this study. It is found from the calculation shown in Fig. 2 that the Ohkawa current is the dominant noninductive current in this plasma. It is also found that there is a large difference between the evaluated noninductive current and the observed total current. This fact shows that the inversely induced current component has a significant role in this plasma. We are interested in
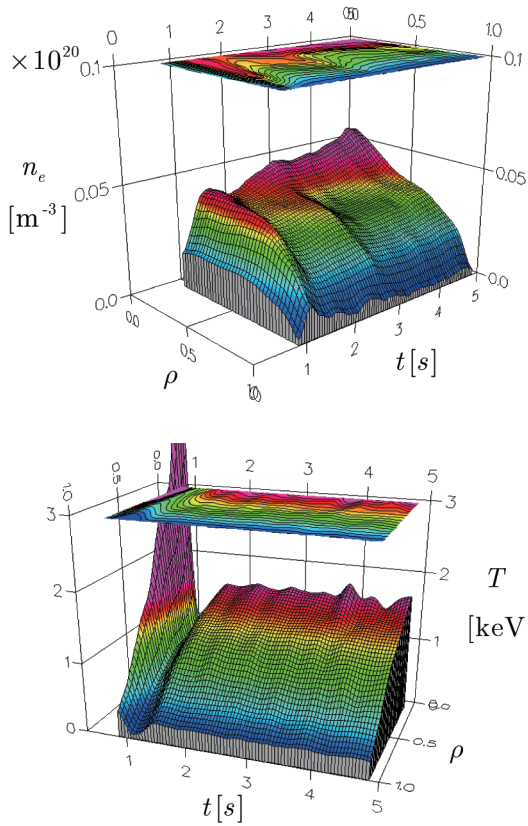
Fig. 1 Experimentally evaluated time evolutions of density and temperature profiles of a low beta NBI plasma in LHD.
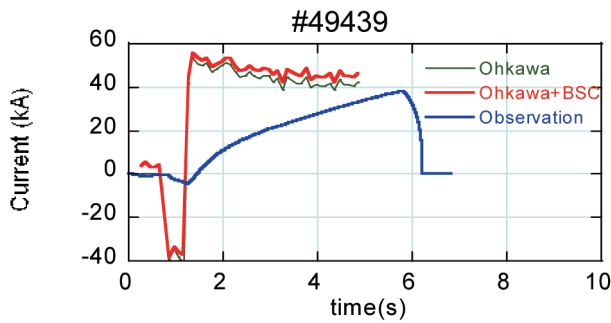

Fig. 2 Time evolution of experimentally observed total current and those of the Ohkawa and bootstrap current estimated by the BSC and FIT codes.

the current density profile in the transient state.

Numerical simulation of the rotational transform is performed using density and temperature profiles evolution shown in Fig. 1. Since the ion temperature is necessary for noninductive current calculation by the BSC and FIT codes, we assume that the ion temperature is equal to the electron temperature. Observed total plasma current shown in Fig. 2 is used as the boundary condition for the equation of the rotational transform. The result is shown in Fig. 3. In this calculation, MHD equilibrium and the noninductive current is re-evaluated every 0.1 s. We also
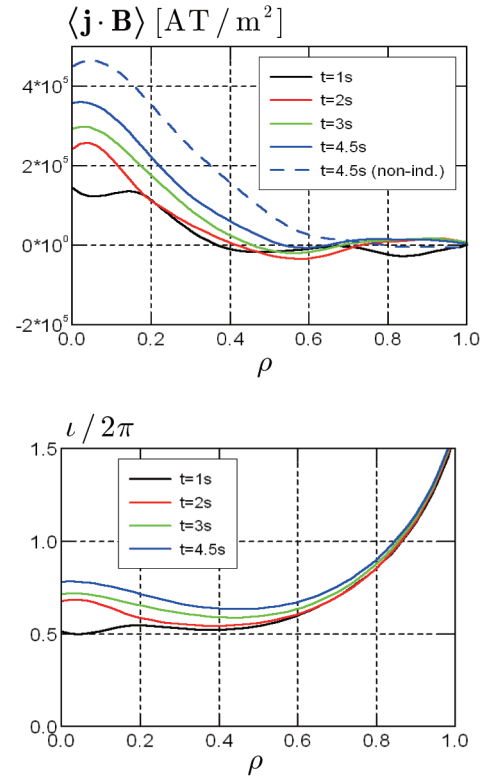

Fig. 3 Time evolutions of current density and rotational transform profile obtained by the numerical simulation.

performed the calculation in which we update MHD equilibrium and noninductive current every 0.01 s, and found that the time interval of 0.1 s is sufficient for this calculation. The dashed line in Fig. 3 shows noninductive current density profile at $t = 4.5$ s. Although the total current density increases gradually to the value of the noninductive one, inductive current component is not small even at $t = 4.5$ s. The rotational transform at $\rho = 0.5$ is about 0.67 at $t = 4.5$ s. This value of the rotational transform is close to that evaluated by the Motional Stark Effect (MSE) measurement [3]. The value estimated using noninductive current density profile is about 0.75. In this simulation, we used the neoclassical electric conductivity calculated by the BSC code. The use of Spitzer conductivity results in a slower time evolution of the rotational transform. Figure 4 shows the ratio of neoclassical electric conductivity and classical Spitzer conductivity. Significant reduction of the electric conductivity due to the neoclassical effect can be seen. This tendency agrees roughly with the simple estimation obtained using the trapped particle fraction [7]. We will use the neoclassical conductivity for the calculation in Sec. 4.

4. Analysis of Plasma Current in a Super Dense Core Plasma

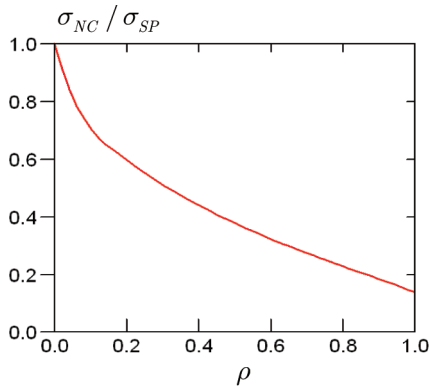In LHD, a superdense core (SDC) mode can be achieved with an internal diffusion barrier (IDB) [8]. In

Fig. 4 Ratio of neoclassical electric conductivity and classical Spitzer conductivity.

this mode, a superdense plasma with the central density of $\sim 5 \times 10^{20}\,\mathrm{m}^{-3}$ is maintained by the formation of an IDB with extremely high density gradient. In order to clarify the physics of SDC plasma formation, it is very important to know the rotational transform profile in such plasmas [8]. Since the rotational transform is very sensitive to the plasma current, consistent analysis of both noninductive and inductive currents to the MHD equilibrium is necessary. As shown in the previous section, time history of plasma parameters is important to estimate the inductive current and rotational transform profiles accurately.

Typical density and temperature profile evolution of SDC plasmas obtained by the Thomson scattering measurement are shown in Fig. 5. The high density plasma whose central electron density reaches over $4 \times 10^{20}\,\mathrm{m}^{-3}$ is produced by a series of pellet injections, and the superdense core is formed from $t \sim 0.8\,\mathrm{s}$ in this case [8]. The volume averaged beta of this high density plasma estimated by the diamagnetic measurement is $\langle \beta_{dia} \rangle = 0.5 \sim 1.0\%$. Before pellet injections, plasma beta is low ($\langle \beta_{dia} \rangle \sim 0.2\%$), noninductive current is mainly driven by the NB injection, and the Ohkawa current calculated by the BSC and FIT codes is about 200 kA. However, observed total current at this period is less than 20 kA. After pellet injections, the bootstrap current becomes the dominant noninductive current, and it is estimated to be about 50 kA. The observed total current is less than 25 kA.

The time evolution of the noninductive current $\langle J_{NI} \cdot B \rangle$ profile obtained by the BSC and FIT codes is shown in Fig. 6. Before pellet injections, noninductive current density profile due to the Ohkawa current is peaked at the center. After pellet injection, the central density is increased, and the central temperature is decreased. This causes a rapid drop in the Ohkawa current due to fast thermalization of fast ions produced by the NB injection. After that, the broader noninductive current profile can be seen because of the bootstrap current. It can also be seen from this figure that the bootstrap current increases after the density drops and the temperature recovers, i.e., the
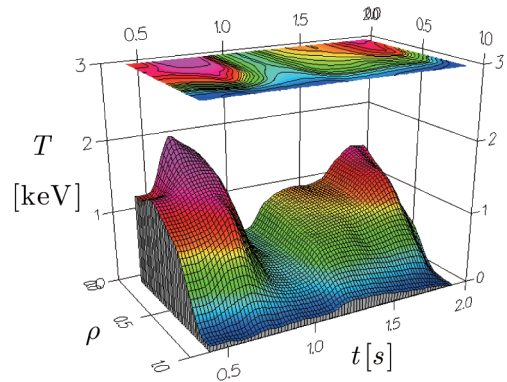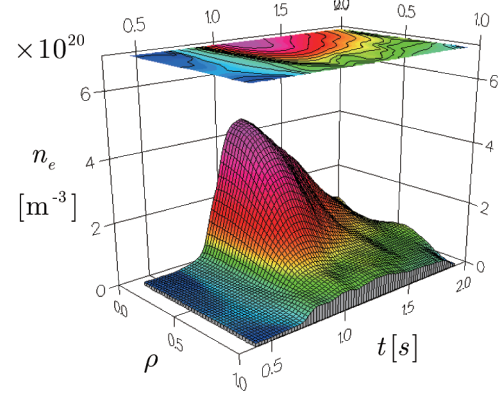

Fig. 5 Experimentally evaluated time evolutions of density and temperature profiles of an SDC plasma.
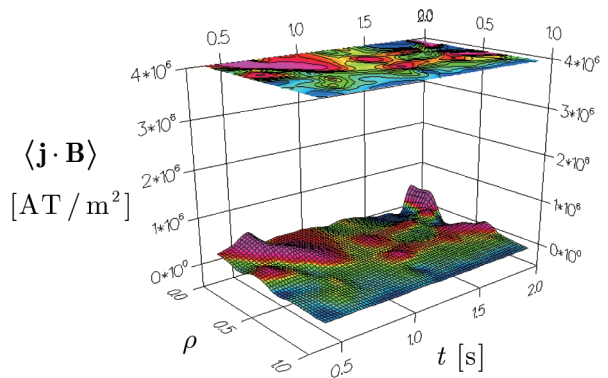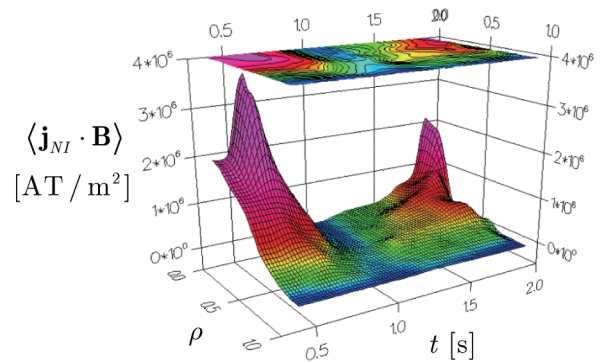

Fig. 6 Time evolution of the calculated parallel noninductive current density and total parallel current density in an SDC plasma.
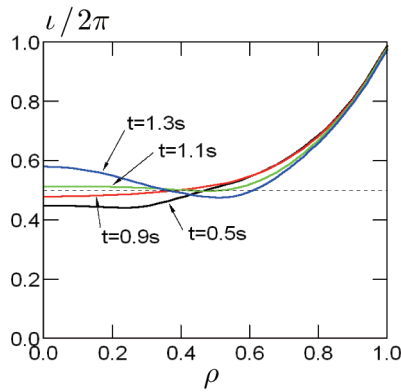
Fig. 7 Time evolution of the calculated rotational transform profile in an SDC plasma.

collision frequency decreases. Time evolution of the parallel current $\langle \boldsymbol{J} \cdot \boldsymbol{B} \rangle$ calculated by TASK/EI is also shown in Fig. 6. In this calculation, experimentally obtained density and temperature profile shown in Fig. 5, equilibrium quantities, and noninductive current calculated by the BSC and FIT codes are updated every 0.1 s self consistently. The boundary condition, i.e., the total plasma current, is given by the experimental data. It is clearly seen that the inductive component of the plasma current almost cancels the noninductive current, and the net toroidal current is significantly reduced. Resultant evolution of the rotational transform profile is shown in Fig. 7. Double $\iota = 1/2$ surfaces appear around the half radius. These profiles are similar to those in current-free MHD equilibria.

In order to evaluate the effect of the time interval between subsequent equilibrium and noninductive current calculations, we also performed a calculation in which we update MHD equilibrium and noninductive current every 0.01 s. Even though there is a small difference between the result from the calculation with time interval of 0.1 s and that of 0.01 s, especially at the beginning of the calculation, they agree well with each other. Therefore, we can conclude that the time interval of 0.01 ∼ 0.1 s seems sufficient for the validity of our assumptions in the equation of ι evolution for the calculation of LHD plasmas.

5. Summary

We have developed a net plasma current simulation code for integrated simulations of helical plasmas, and analyze net plasma currents observed in LHD plasmas. The effect of the inductive current is important for estimating the net plasma current, especially when the beam driven

currents are considered. Numerical analysis for a low beta NBI heated plasma shows that it takes more than 4 s for the toroidal plasma current (or rotational transform) profile to reach the steady state. If we estimate the characteristic current diffusion time using the electric conductivity at the half radius, it is about 2.5 s. However, it is strongly dependent on the electron temperature and takes more time to reach the steady state at the plasma center. On the other hand, the characteristic L/R time for the total current ramp up is estimated as about 5 s from the experiment. It is comparable to the current diffusion time. This fact suggests that both the current diffusion and L/R times contribute to determine the time scale of the current density profile evolution. It is also shown that the neoclassical correction of the electric conductivity is important. In an SDC plasma that we analyzed, net toroidal current is negligible due to the inductive component, although the noninductive current is significantly large. Despite this, noninductive current, especially the bootstrap current, will become important if we consider long pulse SDC shots or SDC reactor scale plasmas. For most LHD plasmas, time interval of 0.1 s between subsequent MHD equilibrium and noninductive current calculations is sufficiently small for the validity of the numerical assumption unless the noninductive plasma current changes rapidly.

In the present study, we used experimentally obtained total toroidal current evolution as a boundary condition. In order to perform predictive calculations, however, we should use the loop voltage evaluated numerically as a boundary condition. We should also incorporate the TASK/EI module in the integrated transport simulation code TASK3D. These are our future study subjects.

[1] Yuji Nakamura *et al.*, Fusion Sci. Technol. **50**, 457 (2006).
[2] M. Sato *et al.*, submitted to Plasma Fusion Res.
[3] Yuji Nakamura *et al.*, Proc. of 21th IAEA Fusion Energy Conf. (Chengdu, China, 2006) IAEA-CN-149/TH/P7-1.
[4] S.P. Hirshman and D.J. Sigmar, Nucl. Fusion **21**, 1079 (1981).
[5] S.P. Hirshman, W.I. van Rij and P. Merkel, Comput. Phys. Commun. **43**, 143 (1986).
[6] P.I. Strand and W.A. Houlberg, Phys. Plasma **8**, 2782 (2005).
[7] K.Y. Watanabe *et al.*, J. Plasma Fusion Res. Ser. **5**, 124 (2002).
[8] T. Morisaki *et al.*, Phys. Plasma **14**, 056113 (2007).